Research Square

Preprints are preliminary reports that have not undergone peer review.
They should not be considered conclusive, used to inform clinical practice,
or referenced by the media as validated information.

Sensitivity of reservoirs to sedimentation; Spatiotemporal analysis of the driving forces, implications, and the way forward

Joan Akandi Atulley (akandejoan@gmail.com)
JJ College of Engineering and Technology https://orcid.org/0000-0001-7334-3221
Adjei A. Kwaku
Kwame Nkrumah University of Science and Technology
Charles Gyamfi
Kwame Nkrumah University of Science and Technology
Emanuel D. Owusu-Ansah
KNUST Department of Economics: Kwame Nkrumah University of Science and Technology Department of Economics
Melvin A. Adonadaga
C.K. Turdam university of Technology and Applied Science
Odai S. Nii
Accra Technical University

Research Article

Keywords: Bathymetry, Reservoir, Remote sensing, sedimentation, land-use change, Tono, Vea

Posted Date: March 25th, 2022

DOI: https://doi.org/10.21203/rs.3.rs-1435177/v1

License: This work is licensed under a Creative Commons Attribution 4.0 International License.
Read Full License

Sensitivity of reservoirs to sedimentation; Spatiotemporal analysis of the driving forces, implications, and the way forward

Joan A. Atullley[a*], Adjei A. Kwaku. [a], Charles Gyamfi[a], Emanuel D. Owusu-Ansah[a], Melvin A. Adonadaga[b], Odai S. Nii[c],

a. *Regional Water and Environmental Sanitation Center Kumasi (RWESCK), Civil Engineering Department, Kwame Nkrumah University of Science and Technology, University Post Office, Kumasi, Ashanti Region, Ghana*

b. *C. K. Tedam University of Technology and Applied sciences, Box 24, Navrongo-Ghana*

c. *Accra Technical University, Accra, Greater Accra Region, Ghana*

Abstract

Reservoirs are significant freshwater sources. Meanwhile, reservoir storage is compromised by sedimentation for which reason reservoir sedimentation has become an important matter in reservoir operation and management. This paper aimed to assess land cover change in two catchments in Northern Ghana in relation to the sedimentation of reservoirs located downstream of their catchments. The two reservoirs comprise a small-sized (Vea reservoir) and a large-sized reservoir (Tono). First, bathymetric surveys were performed on reservoirs to calculate the loss of storage capacity between 1985 and 2020. Then satellite imagery from 1986, 1996, 2006, and 2020 was used to classify land cover in catchments for the respective years. The results revealed an annual sedimentation rate of 0.17% and 0.304% for Tono and Vea, hence indicating a higher sedimentation rate in the smaller reservoir (Vea). During the study period, savannah forest decreased from 34.7% to 21.6% in Tono and a more drastic decline from 29.4%(1985) to 9.9%(2020) in Vea. This reduction was largely influenced by the expansion of farmlands from 18.7% to 47.9% in Vea and 19.2% to 39% in Tono. According to these observations, watershed land cover characteristics have a significant bearing on the rate of sedimentation in reservoirs located downstream of their catchments. Morso, small-sized reservoirs are known to be more vulnerable to sedimentation but the severity of sedimentation in them is exacerbated by extensive tree cover removal in their catchments since that would result in higher sediment generation. Hence, adopting a multi-sectorial approach to dealing with vegetation change patterns is necessary to sustain reservoirs' storage.

Keywords; Bathymetry, Reservoir, Remote sensing, sedimentation, land-use change, Tono, Vea

Corresponding author's email; akandejoan@gmail.com

Corresponding author's contact;+233 24 628 1881

1.0 Background

Reservoirs are formed by constructing dams across rivers or streams to impound water. They play vital roles in the world's economy by providing water for aquaculture, irrigation, hydropower, and Domestic water supply among others (Namara et al., 2011). As reservoirs trap runoff, the accompanying sediments are also deposited in the reservoirs reducing their

storage space over time (Dutta, 2016). Reservoir sedimentation has long been seen as a problem to reservoir storage in many parts of the world (Jacobsen, 1997). Reservoir sedimentation has severe consequences for irrigation, flood management services, energy production, water supply and degrades aquatic habitat as sediments build up in reservoirs over time, displace storage volume (Kondolf et al., 2014; Rahmani et al., 2018). Depending on the degree of sediment accumulation, outlet structures may be clogged or damaged generating security problems (Schleiss et al., 2016). Hence sedimentation valuation is becoming an increasingly significant matter in reservoir operation and management (Wang et al., 2005). A review of the literature indicates a broad range of reservoir capacity loss to sedimentation globally ranging from an annual loss of 0.03% in Lake Mead in the United States to 2% for Manwan dam in China (Fu et al., 2008; Smith et al., 1960). The annual average rate of silt deposition in the world's largest reservoir was found to be 0.55 to 1% (Yuan et al., 2015). Also, 1.5% capacity loss is reported for the Tarbela dam in Pakistan (Tate and Farquharson, 2000). In central Europe, a study of 19 reservoirs with storage capacities ranging from 1.5 to 226Mm3 indicated an average annual depletion rate of 0.51% (Glymph 1973). Tono and Vea reservoirs in Ghana are estimated to be losing their capacity at an annual rate of about 0.11% and 0.14Mm^3 respectively (Imagen C., 2013; Adongo et al., 2016). In the Upper East Region of Ghana, Adwubi et al., (2009) found small reservoirs losing their storage space to sediment rapidly at a rate of 1.7%/year with the dead storage space of some small reservoirs already filled up by sediment. Even worse case of full capacity loss was documented for Sweasey Dam in California, where the reservoir was fully infilled by sediment only 31 years of Operation (Mount, 1995).

The gradual process of reservoir storage capacity loss to sedimentation depends on; 1) morphologic factors of the reservoir, 2) The sediment yield of the river or stream on which the reservoir is built, and 3) the operational scheme of a project (SUNDBORG, 1992; Tarela and Menéndez, 1999). Regarding the morphology of reservoirs, small and medium storage reservoirs loss their storage space to sediment more swiftly than larger reservoirs making them more vulnerable to sedimentation (Chanson, 1998; Chanson and James 2005). For example, in a comprehensive reservoir study Dendy et al., (1973), found the following average annual loss rates for different storage capacities; (a) 3.56% for reservoirs with storage capacities less than 0.012Mm^3, (b) 2.0% for reservoirs with a capacity between 0.012 and 0.12Mm^3, (c) 1.02% for reservoirs with a capacity between 0.123 and 1.23Mm^3, (d) 0.81% for reservoirs between 1.23 and 12.3Mm^3, (e) 0.43% for reservoirs between 12.3 and 123.3Mm^3, (f) 0.23% for reservoirs within the range of 123.3 and 1,233.0 Mm^3 and (g) 0.16% for reservoirs above 1,233.3 Mm^3. Suggesting that greater capacity loss rates are observed for smaller reservoirs.
The sediment yield of the stream on which the reservoir is built depends on the characteristics of the reservoir catchment such as the geology, topographic character, climate, geomorphology, hydrology, vegetation type, and land use (Kondolf et al., 2014). Natural land-cover changes influence the rate of runoff and consequently sediment transport

(Harden C.P, 1993; Boakye et al., 2018). For instance, high soil erosion and sediment yield are reported to be associated with cultivated lands, built areas, and bare lands (Crowder, 1987; Molla and Sisheber, 2017) while the presence of tree vegetation is linked to the low rate of particle transfer (Boakye et al., 2018) and subsequent sediment deposition into reservoirs. Several studies the world over has reported extensive transition of land use to farmlands and built areas at the expense of forest cover (Guan et al., 2011; Ottinger et al., 2013; Gebremicael et al., 2013; Awotwi et al., 2014; Opoku et al., 2019), indicating a likelihood of higher runoff and consequent higher sediment generation in the future. Given the linkage between catchment landscape modification and sedimentation (Walling, 1999) and the fact land cover change is inevitable as growing humans are dependent on the natural land, it is necessary to ascertain the extent of reservoir catchments' land-use change from the time of reservoir construction. This would offer an essential foundation to understanding the complex relationship between catchment physiographics and sediment deposition dynamics to inform policy and guide practical decisions towards sustainable management of water resources. The objective of this study, therefore, is to evaluate Tono and Vea reservoirs' catchment land-use change and determine the sedimentation rate of these reservoirs from1985 to 2020. The study also proposed mitigation actions to inform policy and watershed management practice. The study used Remote Sensing (RS) and Geographical Information System (GIS) techniques in data acquisition and processing as its the commonest technique widely used by researchers for analyzing earth system functions and detecting Spatio-temporal LULCC (Sawaya et al., 2003; Mallick et al., 2008).

2. Study Area

Tono and Vea are located in the northeastern part of Ghana between latitude 10.910245^{o} and 10.878133^{o} and longitude -1.152733^{o} and -0.838613^{o} respectively. Both dams were completed in 1985 with dam wall lengths of 3,500m and 1,600m; dam wall height of 18.6 and 13.5; storage capacities of 93 Mm^3 and 17.22Mm^3. The catchments feeding these reservoirs are 650km^2 and 305km^2 respectively, extending across into neighboring Burkina Faso (IDA, 1978). The Tono reservoir is fed by the Tono river while the Yarigatanga river feeds the Vea reservoir. Tono reservoir is the largest earth in Ghana (Namara et al., 2011). Tono and Vea are important water resource assets to the Upper East Region as they are the main source of water for irrigation, aquaculture, construction, and municipal water supply among others (Venot et al., 2012).

The study domain is a savanna ecological zone characterized by significant temperature variations and a unimodal, unpredictable rainfall pattern with three seasons; Rainy season (July to September), Dry season (February to May), and Hamatan season (November to January) (Barry, et al., 2005). The main soils types found in the area include vertisols, luvisols, lithosols, and arenosoles and the average annual rainfall varies from 800mm to 1240 mm with the highest rainfall (more than 80%) experienced during the rainy season

(July to September)(Mul et al., 2015). Agriculture is the main economic activity in the Tono and Vea catchments and includes rain-fed agriculture, irrigated agriculture, livestock production, and aquaculture. Fig 1. shows the location of Tono and Vea and surrounding farming communities.

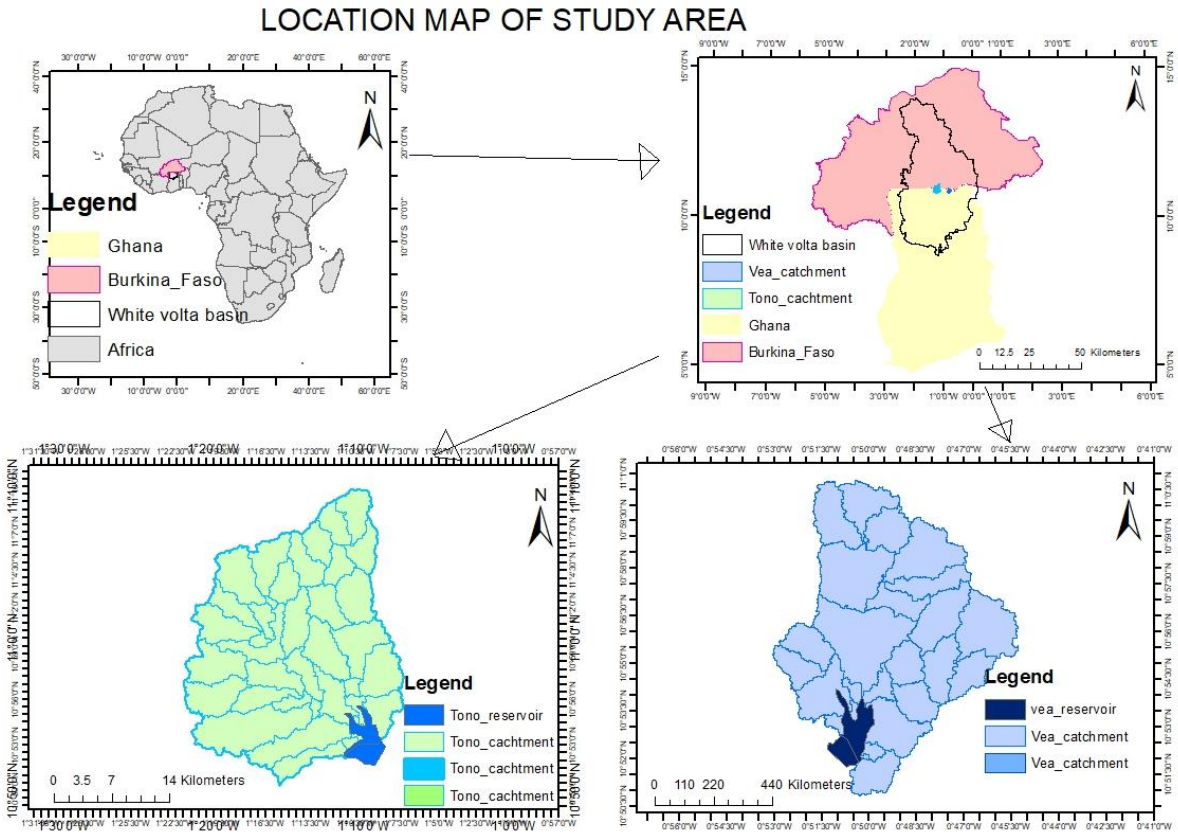

Fig 1. Location of Tono and Vea reservoirs and catchment

3. Materials and Methods

Primary and secondary data were used in this study. Primary data was collected through a bathymetry survey and informal interviews while the secondary information was Landsat images obtained from the USGS site as well as published and unpublished sources including articles, reports, diaries, and records. Following data collection, most of the preprocessing and analysis of both bathymetry and satellite data were executed using GIS software. The entire data acquisition, processing, and analysis procedures were performed following the underlying flow chat in fig 2.

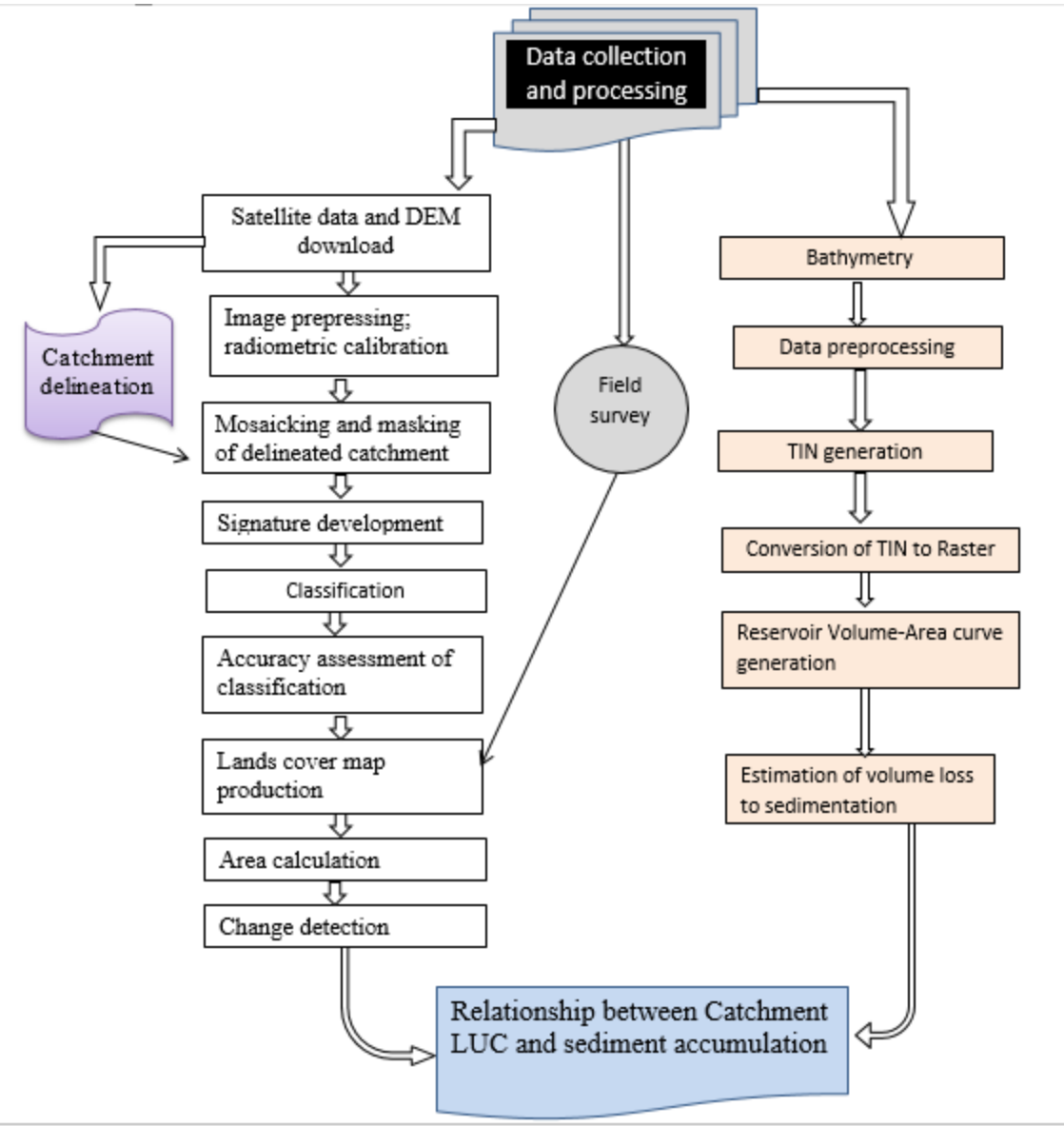

Fig. 2 Data acquisition and analysis flow chat

Note; Left column is for processing the land cover data and the right column is for processing reservoir sedimentation data

3.1 Bathymetric survey

To understand the linkage between sedimentation and LULCC, the current state of reservoir sedimentation was first estimated by conducting a bathymetry survey on Tono and Vea reservoirs in November 2020. Depth measurement was collected using GARMIN echoMAP CHIRP 72SV mounted on the canoe. Water depth was measured at an accuracy of ±0.01m as the canons navigated along 30m interval lines. XYZ data points obtained from the survey were used to generate a Triangulated irregular model (TIN) with the Delaunay triangulation

method so that all points are connected using their two nearest neighbors to form triangles (Wilson and Richards, 2006). The current storage capacity of Tono and Vea was computed using the storage capacity tool in the special analyst supplemental extension tool.

The bulk volume of sediments accumulated (BVs) in m^3/yr and mean annual rate of sedimentation (ArS) in % was computed from equation1 and 2.

$$\text{BVs} = \textit{Initial storage capasity} - \text{Current storage capacity} \quad (1)$$

$$\text{ArS} = \frac{\textit{Initial storage} - \textit{final storage}}{\textit{Age of reservoir}} * 100 \quad (2)$$

Note the Current storage is the storage capacity obtained from the bathymetry survey

3.2 Field survey and interviews

Field survey was conducted and specific latitude and longitude of land use categories were taken. These points together with Google earth maps were used for validation of the LULC classification. Also, informal interviews of elderly local people, management of Irrigation Company of the Upper Region (ICOUR), Forestry Commission, and Ministry of Food and Agriculture (MoFA) were conducted to obtain direct field knowledge about the trend of land cover changes in the area. From the field survey and interviews, land use was categorized into 5 classes (water, savannah forest, open savanna, farmlands, and built areas). Based on the above land use categories, land-use class maps were produced for 1986, 1996, 2006, and 2020.

3.3 Secondary data collection

An important consideration for monitoring land cover change (LCC) is the temporal frequency of remote sensor data acquisition required to characterize change events adequately. The data type and temporal frequency applied for change analysis vary broadly since ecosystem conditions and change is not uniform across the globe. For instance, Lunetta et al., (2004) reported a 3-4 years nominal temporal frequency as appropriate for North Carolina since the forest undergoes rapid rates of revegetation. While Akubia et al., (2020) 9 years temporal frequency in Southern Ghana, Kundu et al., (2017) and Karamage et al., (2016) used 10 years frequency in Madhya Pradesh, India, and Rwanda respectively. Cycles of depopulation and repopulation of farmlands influence patterns of deforestation and regeneration of adjacent savannah woodlands in Northern Ghana and Burkina Faso, resulting in a relatively low change rate (Wardell et al., 2003). Hence, a longer period frequency is required to minimize change commission and omission errors. Thus, to analyze the trend of land cover in Tono and Vea catchments, 10yrs temporal frequency was used.

High-resolution imagery provided by sensors such as Worldview-2 would have been preferred but images from Landsat archives was considered for this study. Though low-

resolution imagery, the choice was informed by the fact that, Landsat imagery is the most common earth observation data source, less costly to acquire and their analysis needs much less computing resources. Specifically, Landsat 8 data was used because it has been proven to be the most accurate, relative to other Landsat collection and appropriate for time series analysis (Poursanidis et al., 2015), but since Landsat 8 was only launched recently, data for the earlier study years could not be obtained. Hence, for the Years 1986,1996, and 2006, the Landsat 5 Thematic Mapper (TM) images were used. While Landsat 8 OLI/TIRE was acquired for 2020. Images were downloaded from the USGS (United States Geological Survey) official website (erthexplorer.usgs.gov). The reservoirs catchments extend beyond a single tile; hence two images each for the years under study were preprocessed and mosaicked in other to extract the study catchments. The 1995 image was merged with a 1996 image because of the unavailability of quality pair from 1996. Characteristics of the data are shown in table 1.

Due to the desire for cloud-free images, data was acquired for the dry season (December to April) but the unavailability of data for the same season for all study years required that some data be obtained for different seasons. Consequently, land cover maps generation was challenged by the confusion of spectral responses from different features. Particularly, the spectral mixing of different surface elements due to seasonal variability in vegetation cover types and soil moisture conditions.

Table 1; Details of acquired satellite data used in the study

Satellite id	Sensor id	Path/row	Acquisition date	Spatial resolution	Quality/ Cloud cover
Lansat 5	TM	194/52	1986-11-27	30 m	9/2
Lansat 5	TM	194/53	1986-11-27	30 m	9/2
Lansat 5	TM	194/52	1995-06-29	30 m	7/2
Lansat 5	TM	195/52	1996-03-02	30 m	7/2
Lansat 5	TM	194/52	2006-11-02	30 m	9/3
Lansat 5	TM	195/52	2006-11-09	30 m	9/2
Lansat 8	OLI/TIRS	194/52	2020-05-16	30 m	9/2.19
Lansat 8	OLI/TIRS	195/52	2020-05-23	30 m	9/2.42

Landsat 8 level 1 data products used in this study typically include data from both the operational land imager(OLI) sensor and the thermal infrared sensor(TIR). Landsat 8 OLI/TIR and 5TM are obtained from different sensors built within the same satellite system with a nominal spatial resolution of 30m and an approximate scene size of 170km north-south by 183km east-west (USGS, 2021). Landsat 5TM images consist of seven spectral bands with a 120 meters spatial resolution for band 6 (Thermal Infrared) but resampled to a 30-meter pixel. Landsat 8 OLI/TIRS provide enhancement in overall image quality, the

number of spectral bands, and their spatial resolution from prior Landsat images (Poursanidis et al., 2015). OLI sensor provides two additional spectral bands: a deep blue visible channel (band 1) with a shorter wavelength (0.43-0.45µm) specifically designed for water resources and coastal zone investigation, a new infrared channel (band 9), covering a very short range of wavelengths in the short-wave infrared (1.36-1.39µm) for the detection of Cirrus clouds (USGS, 2020).

3.3.1 Satellite data preprocessing (Radiometric correction)

The measurement of signals by satellite is affected by the presence of gases, solid and liquid particles hence, the atmospheric effects on images were corrected following López-serrano et al., (2016) to improve the accuracy of the classification. Radiometric correction (RC) is important to improve the interpretability and quality of the remotely sensed data. It is particularly important for the current study that compare images from different sensors and different times (Chander et al., 2009). Sensors record the intensity of electromagnetic radiations for each pixel as digital numbers (DN) which usually includes radiations scattered and emitted by particles in the atmosphere. Meanwhile, in satellite image analysis, actual surface values are of interest. The actual surface values comprise, reflected, or emitted radiations from the surface. Hence the main purpose of RC is to calibrate the pixel values and correct for errors in the values, thus, converting DN in the image to Top of atmospheric (TOA) reflectance (true ground reflectance) values. The benefits include, using the TOA Reflectance removes the cosine effect of different solar zenith angle due to time difference in data acquisition. TOA Reflectance also compensates for different values of exoatmospheric solar irradiance arising from spectral band difference, and also correct for the variations in earth-sun distance between data acquisition and dates.
Generally, radiometric calibration involves two steps but differs with sensors.

Calibration of Landsat Multispectral Scanner (MSS), TM, Enhanced Thematic Mapper (ETM) is achieved through equations 3 and 4
Step 1; Converting DN (Qcal) in the raw data to radiance (L_λ) based on rescaling factors provided in the metafile of the satellite data

$$L_\lambda = \left(\frac{LMAX_\lambda - LMIN_\lambda}{Q_{calmax} - Q_{calmin}}\right)(Q_{cal} - Q_{calmin}) + LMIN_\lambda \qquad (3)$$

Where L_λ- spectral radiance at the sensor's aperture
Q_{CAL}- Quantized calibrated pixel value
Q_{calmax} -Minimum quantized calibrated pixel value (corresponding to $LMAX_{\lambda,\ for}$ Landsat TM =255)
Q_{calmin}-Minimum quantized calibrated pixel value (corresponding to $LMIN_\lambda$, for Landsat TM=1)
$LMAX_\lambda$-Spectral at sensor radiance that is scaled to Q_{calmax}
$LMIN_\lambda$-Spectral at sensor radiance that is scaled to Q_{calmin}

Step 2; Converting sensor spectral radiance (L_λ) to TOA reflectance (ρ_λ)'

$$\rho\lambda = \frac{\pi \bullet L_\lambda \bullet d^2}{ESUN_\lambda \bullet cos\theta s} \quad (4)$$

Where L_λ-Radiance computed in equation 1

d^2 -Distance between earth and sun on the day of collection "squared"

$ESUN_\lambda$ -Exoatmospheric irradiance (value found in the Landsat Handbook)

$Cos\theta$ -Solar zenith angle in radiance (90-Sun Elevation) and converted to radiance from degrees

Calibration of Landsat 8 OLI/TIR is achieved through equation 5 and 6

Step 1; Converting DN to TOA planetary reflectance (not corrected for sun angle)

$$\rho\lambda = M_\rho Q_{cal} + A_\rho \quad (5)$$

Where; $\rho\lambda$-TOA planetary reflectance

M_ρ – Band specific multiplicative rescaling factor from the Metadata file (REFLECTANCE_MULT_BAND_X)

Q_{cal} Band specific additive rescaling factor from Metadata file (REFLECTANCE_ADD_BAND_X)

A_ρ –quantized and calibrated standard pixel value (Digital number) for the wavelength

Note x is the wavelength band being corrected (1,2,3----)

Step 2; Correction for sun angle to get TOA Reflectance

$$\text{TOA Reflectance} = \rho\lambda' \bullet \cos(\theta_{SZ}) \sin(\theta_{SE}) \quad (6)$$

Where $\rho\lambda$' - TOA planetary reflectance

θ_{SE}-Sun Elevation angle (provided in the MTF as SUN_ELEVATION)

θ_{SZ}-Local solar zenith angle; 90^o-θ_{SE}

Radiometricaly calibrated Landsat 5TM and Landsat 8 OLI/TIR are presented visually in Fig.4 for Tono and Vea catchments.

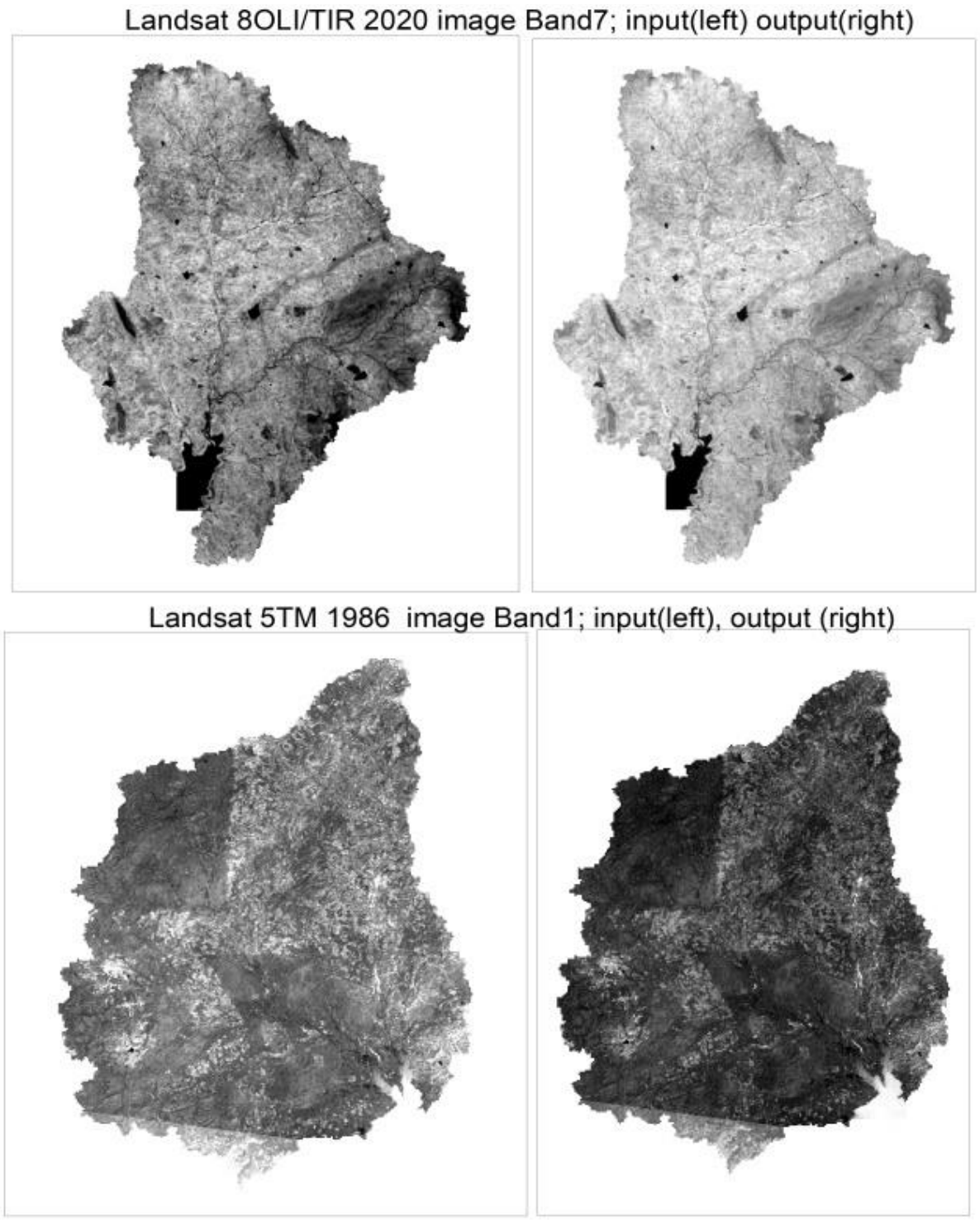

Fig 4; Illustration of radiometric calibration of Landsat 8 OLI/TIR masked to Vea catchment (Top) and Landsat 5TM masked to Tono catchment (bottom). For each image, the Input with DN is to the left while the corrected output image with TOA Reflectance is to the right

After calibrating each band, composite images were formed and the two images for each of the years were mosaicked and both catchments masked out for image classification and

analysis. The radiometric correction process was executed using the raster calculator in the spatial analyst tool.

3.3.2 Classification and LULC change detection

The supervised maximum classification method used in this study is the commonest method in remote sensing image data analysis. it uses the means and variance of training data to estimate the probability that a pixel is a member of a class. The pixel is then placed in the class with the highest probability of membership (Ozesmi and Bauer, 2002). The classification scheme was developed based on the characteristics of the area (Table 2). Longitudes and latitudes of specific land use categories were taken from the field and based on the characteristics of the area, training samples for the 5 land-use classes were drawn and signature files were created. Following the development of signature files, the final step was image classification where the maximum likelihood method was applied to land cover maps generated.

After classification, the magnitude change, percentage change, and annual rate of change for each land-use class was computed from equation 7, 8 and 9

$$\text{The magnitude of change} = \text{Magnitude of the new year} - \text{magnitude of the previous year} \quad (7)$$

$$\text{Percentage change} = \frac{\text{Magnitude of change}}{\text{base year}} \text{X } 100\% \quad (8)$$

$$\text{Annual Rate of Change} = \frac{\text{Magnitude of change}}{\text{No.Years}} \quad (9)$$

Table 2; Classification scheme used for supervised classification

Code	Land cover type	Description
1	Built areas (BA)	villages, towns, artificial infrastructure, roads
2	Farmland (FL)	cropland and grasslands, fallow lands
3	Savannah forest (SF)	Forest reserves, Forest plantation, Scrub forest
4	Savannah woodlands (SWL)	degrade forest, scattered trees, and shrublands
5	Water (W)	perennial ponds, reservoirs, and rivers

3.3.3 Accuracy assessment

Due to the uneven distribution of data in the maximum likelihood classification, many pixels are often misclassified. Classification accuracy was therefore checked by comparing the classified image with ground truth data from field data and the original Landsat image. 15 to 25 random points were selected as reference values for each classified image with every point having a specific color tone and pixel values which were recognized when the data set was trained during the supervised land use classification. All randomly generated points were identified and assigned in different classes and stratified random sampling was used to calculate the accuracy of the classification of each image. From the reference and classified data, three matrices (users' accuracy, producer accuracy, and total accuracy), as well as Kappa statistics, were generated and the results are presented in tables 6-9. The

Kappa coefficient (Kp) has an added advantage of taking into account the misclassified pixels (error of commission and omission) as well.
From the error matrix, the overall accuracy (OA) was calculated by dividing the sum of entries that constitute a major diagonal by the total number of examined pixels, computed mathematically by equation 10

$$OA = \frac{N \sum_{i=1}^{r} X_{ii}}{N^2} \qquad (10)$$

The Kappa coefficient is computed by multiplying the total number of reference points by the sum of the correctly classified pixels, then subtracts the sum of all the class row totals times the class columns totals. The result is then divided by the square of the total number of reference points and subtracts the sum of all the class row totals times the class columns totals. It is estimated mathematically by equation 11

$$Kp = \frac{N \sum_{i=1}^{r} X_{ii} - \sum_{i=1}^{r} (X_{i+} * X_{+i})}{N^2 - \sum_{i=1}^{r} (X_{i+} * X_{+i})} \qquad (11)$$

Where N-Total number of sites in the matrix
r- Number of rows in the matrix
Xii-number in row i and Colum i
X+i- is the total for row i
Xi+ - is the total for column i

4. **Results**

4.1 Sedimentation rate from 1985-2020

The TIN models produced from the 2020 bathymetric survey are presented in Fig 3. Depths of reservoirs range from 0.3m to 15.4m Tono and 0.2m to 12.5m in Vea with the deepest parts located towards the edge of the dam walls.
The bathymetry reveals a current storage capacity of 86.59 Mm^3 and 15.40 Mm^3 for Tono and Vea respectively. Meanwhile, the initial storage capacity at FSL was about 92.6Mm^3 and 17.22Mm^3 respectively (IDA), 1978). This implies that the total bulk volume of accumulated sediment after T=35(1985-2020) years is 5.41 Mm^3 and 1.8247 Mm^3, representing 5.88% and 10.59% for Tono and Vea respectively. Thus, the annual rate of sedimentation which translates into a rate of storage capacity loss is 0.155 Mm^3 (0.17%) and 0.052Mm^3(0.304%) for Tono and Vea respectively. Even though the amount of sediment generated per drainage area over the 35 years is larger for Tono (5.41 Mm^3) than Vea (1.8247 Mm^3,), the percentage decrease in reservoir storage is relatively smaller for Tono (5.88%) compared to the Vea reservoir (10.59%). Thus, the Vea reservoir is more vulnerable to sedimentation losing storage space at an annual rate of 0.304% while Tono reservoir silt at a rate of 0.17%. The trend of annual loss rate shows that the larger reservoir has a lower sedimentation rate while the smaller one has a high sedimentation rate.

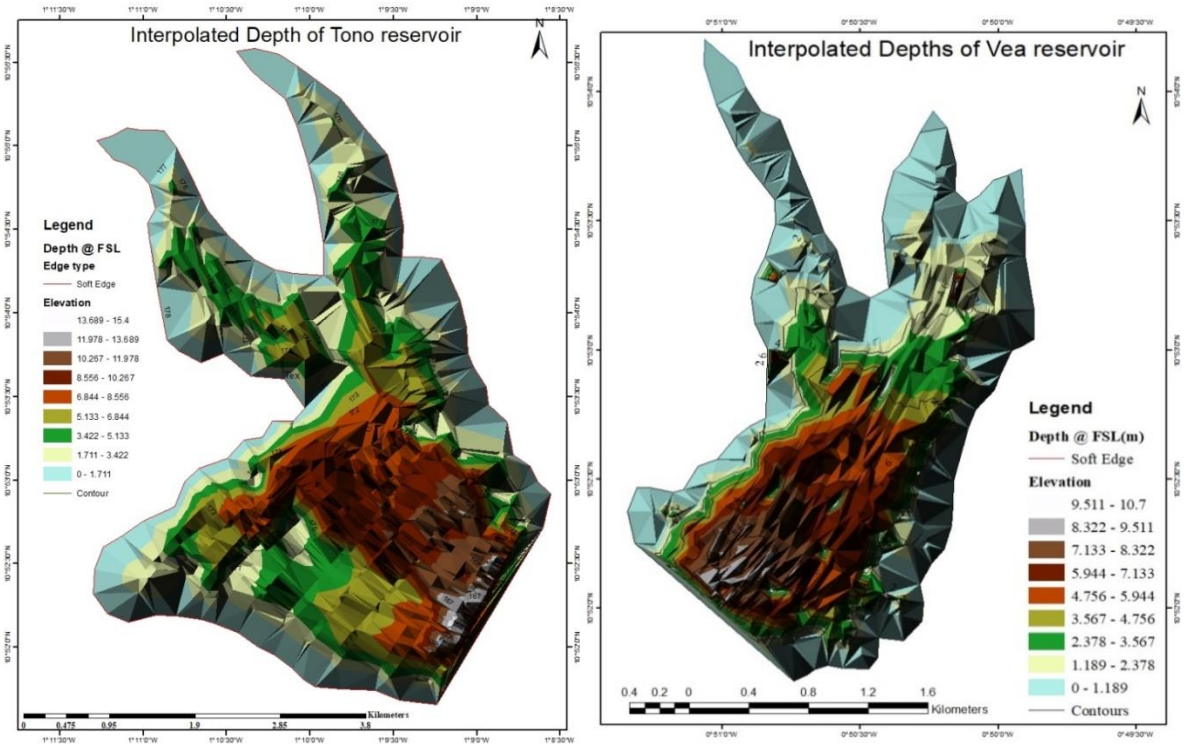

Fig. 3; Bathymetric TIN maps showing the spatial distribution of depth in Tono and Vea Reservoirs

Note; FSL-Full supply level

4.3 Land use pattern in Tono and Vea catchment from 1986 to 2020

Land use maps derived from the classification as well as their respective statistics are presented in Fig 4,5, and 6. Five land use categories were identified and presented in the land use map, including; savannah woodland (SWL), savannah forest (SF) built areas (BA), farmlands (FL), and water (W). The highest land use category from the image classification is Savannah forest and the least is water for both watersheds. Farming activities in the 1980's and 1990's land-use patterns were visible around the settlements but extended to savannah forested areas in 2006 and further around the water bodies in 2020 (Fig 4 and 5). The land-use statistics show that the highest land use category in 1986 covers about 266.4km^2 and 57.0km^2 representing 42.4% and 40.3% of catchment areas for Tono and Vea respectively (fig 6). This was followed by Savannah forest with 217.6km^2 (34.7%) and 41.6 km^2 (29.5%) respectively.

The data suggest that savannah woodlands in the Tono catchment saw a steady decline from 266.4km^2(42.4%) in 1985 to 207.3 km^2 (33%) in 2020 while savannah forests declined from 217.6 km^2 (34.7%) to 135.8 km^2 (21.5) over the same period respectively (Fig 6). This decline can mainly be attributed to the gradual increase in farmlands from 120.7 km^2 (19.2%) in 1986 to 245.0 km^2 (39%) in 2020. Similarly in the Vea catchment, Savannah woodland and Savannah forest cover declined sharply from 40.3% in 1986 to 26.8% in 2020 and 29.4% in 1986 to 9.9% in 2020 respectively, in response to the drastic increase of agricultural lands from 26.5km^2(18.7%) to 67.7km^2(47.9%) over the same period. The

increase in farmlands is linked to increased youth participation in agriculture and a shift from subsistence farming to commercial agriculture. Apart from farmland and built areas expansion, the decline in woodlands can partly be attributed to seasonal burning and illegal logging activities of communities for firewood and charcoal (FSD, 2015). As of 2020, savannah woodland and forest together still cover about 54.6% of Tono Reservoir watershed and 35.8% of Vea reservoir watershed. Signifying that, there is a more rapid increase in farmlands and associated more drastic decline in forest cover in the Vea catchment than in the Tono catchment from 1986 to 2020. The relatively less degradation in Tono catchment tree cover is attributable to the rapid regeneration of adjacent savannah woodlands in Ghana and Burkina Faso (Wardell et al., 2003) as well as the presence of the highly restricted Nzinga natural forest noted for its natural regeneration potential, and several reforestation projects implemented with great success (Fries, 1991; J. Fries and J.Heermans, 2014; Qasim et al., 2016).

Built areas increased from 19.3 km^2 (3%) in 2006 to 30.0 km^2 (4.8%) in 2020 in the Tono catchment and 12.1 km^2 to 18.7 km^2 in Vea catchment for the same period respectively (Fig 6). Water in the Tono catchment declined marginally from 12.4km^2 in 1986 to 9.5km^2 in 2020 representing 2% and 1.5% of the catchment area respectively (Fig 6 a,b) while Vea water increased from 4.1km^2(2.9) in 1986 to 6.3km^2 (4.4%) in 2006 and declined more drastically from 4.6% in 2006 to 2.1% in 2020. Though the construction of dams and dugouts between 1985 and 2006 under the Ghana Social Opportunity Project (GIDA, 2010) may partly account for the variation in water occurrence in the Vea reservoir, this disparity could largely be attributed to seasonal differences.

Though the classification was successful, the most fundamental drawback of this study is the seasonality and the associated difficulty to distinguish class membership. For instance, low-area farmlands appear as pockets of water in the rainy season image while the drastic reduction in reservoir storage in the dry season image exposes a large proportion of the storage area, appearing as bareland/farmland. Also, the possibility of areas being considered as having a change in land cover, but its actually the same land cover could also result in discrepancies.

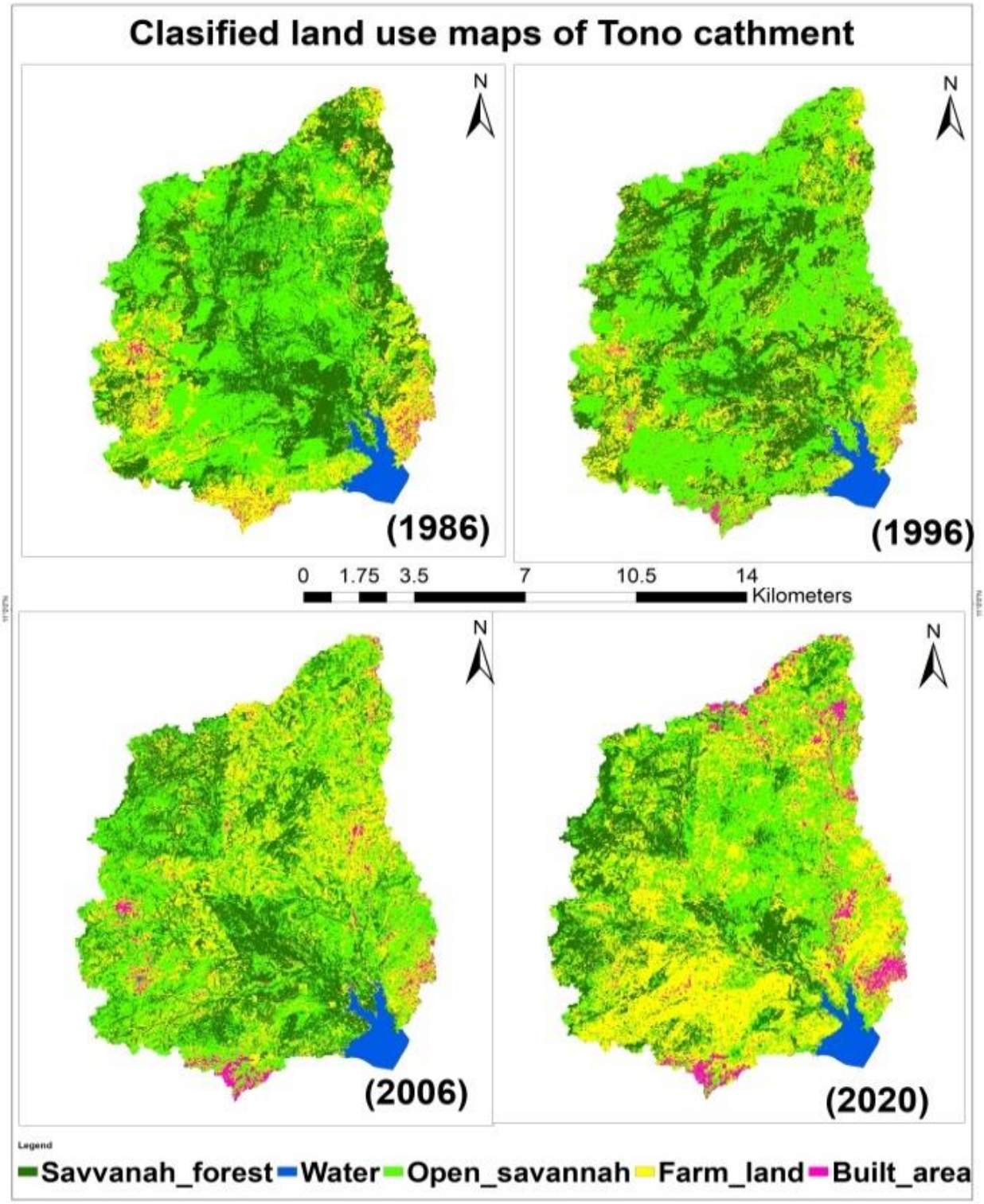

Fig. 4; Land cover Map indicating the different categories of land use in the Tono Catchment for 1986,1996, 2006 and 2020

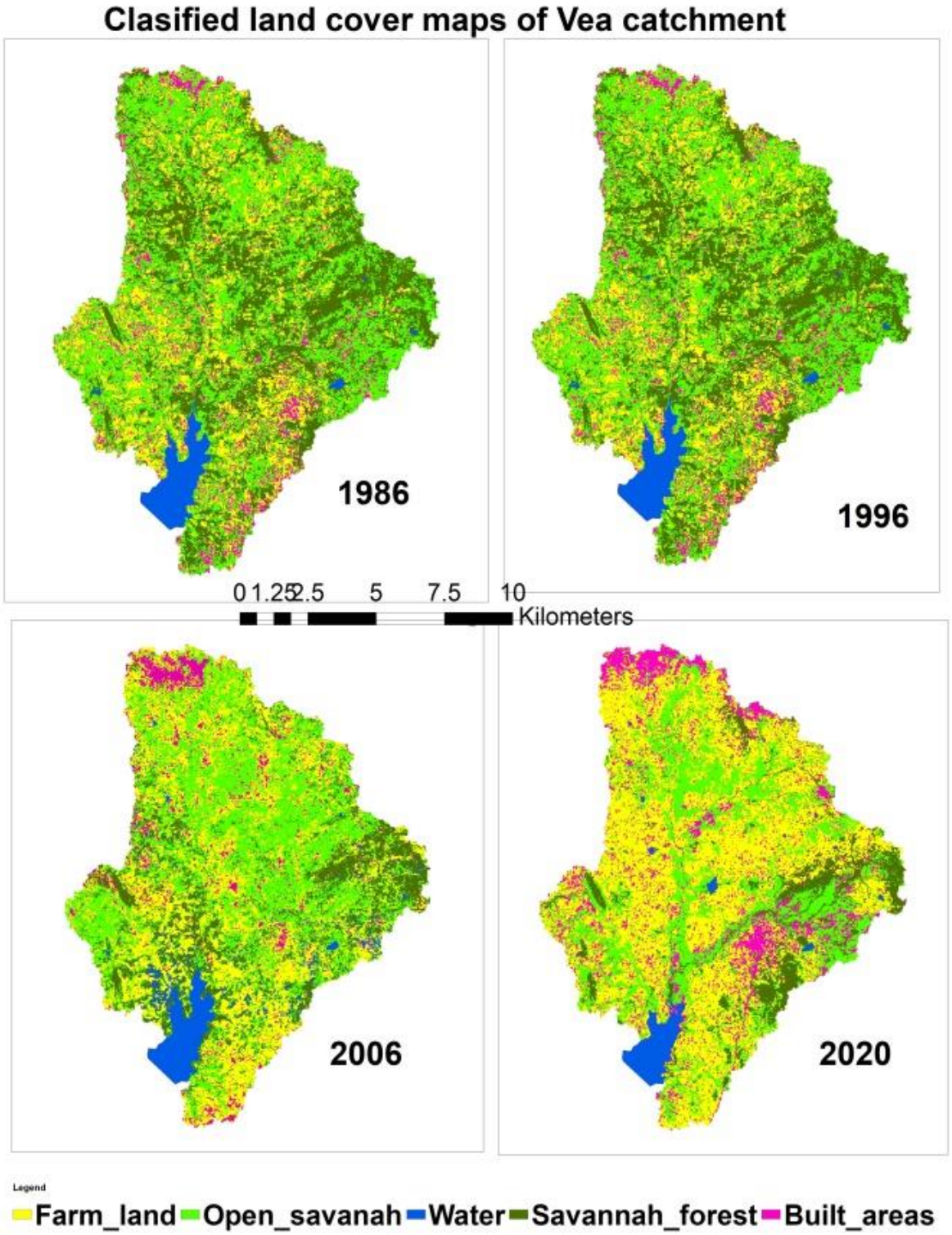

Fig. 5; Land cover Map indicating the different categories of land use in the Vea Catchment for 1986, 1996, 2006 and 2020

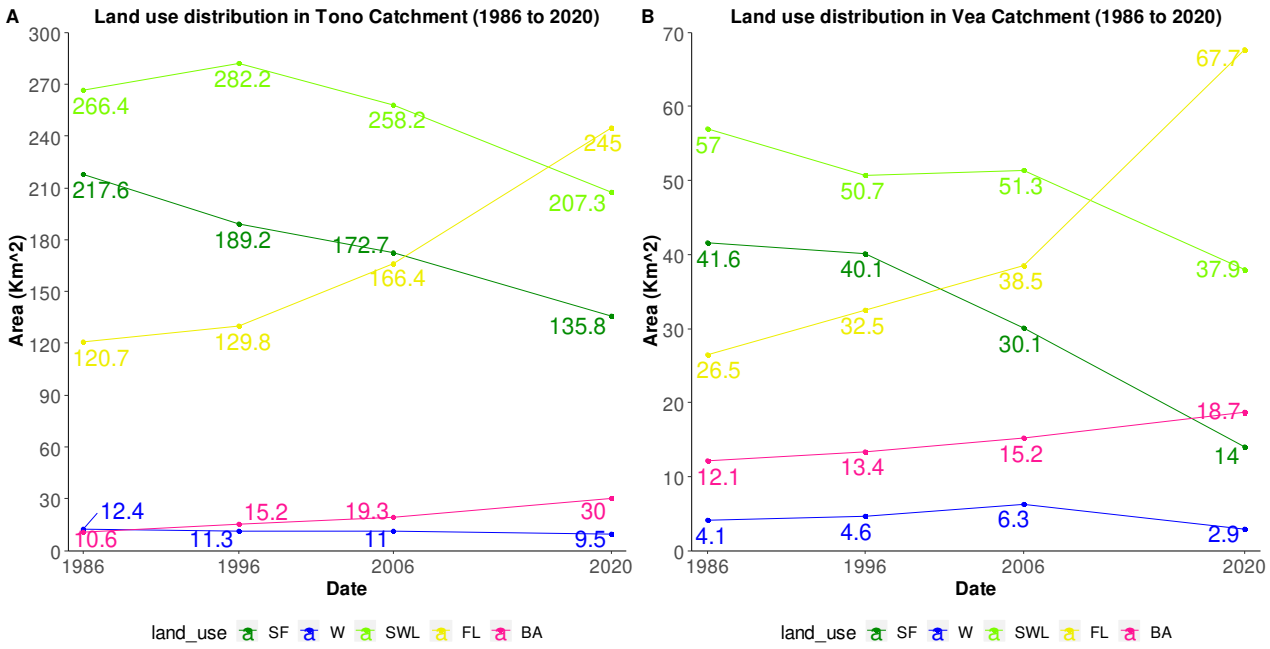

Fig. 6; Comparison of the respective extents of land cover classes by Area of Tono (A) and Vea (B) catchment for the years 1986,1996,2006 and 2020
SWL -savannah woodland, SF -savannah forest BA-built areas, and FL- farmlands W-water

4.3.3 Relative change in land use

The relative change in land use of Tono and Vea catchment was examined based on the land use statistics and presented in Fig 8 x, y and Tables 3 and 4. Land-use changes show a similar pattern in both catchments with farmlands and built areas generally increasing from 1986 to 2020 and savannah forest and savannah woodlands showing a decreasing trend within the same period. Notwithstanding, Tono savannah woodlands increased at an annual magnitude of 42.5 km^2 from 1986 to 1996. This was triggered by the increase in savannah forest depletion at a rate of -13km^2 between the same periods converting them to savannah woodlands. Overall, from 1986-2020, the savannah forest is depleting at an annual rate of -37.6 km^2 while the maximum annual farmlands expansion of 47.2 km^2 (561.2%) was experienced between 2006 and 2020 (Table 3). Though built areas show an increasing trend from 1986 to 2020, the change statistics reveal an annual rate of increase in the magnitude of 5.9km^2 /yr from 1986 to 1996 and declined in the magnitude of change by -8.5% from1996 and 2006 relative to the existing built areas in 1986.
In the Vea catchment, farmlands have increased by 75.9 km^2 between 2006 and 2020 representing 208.7% relative to initial farmland size, while savannah forest has constantly declined greatly at an annual rate of -3.7km^2(-15.4%), 24.9km^2(-99.6), 53.4km^2(-114.8) between 1986-1996; 1996 -2006 and 2006- 2020 respectively (Table 4).

The lowest change in magnitude of water in the Tono catchment is -3% representing 4.4% between 1996 and 2006 and the highest annual change is -13.7 representing -10.8% between 2006 and 2020 (Fig 8x). On the other hand, surface water storage in the Vea catchment increased at an annual rate of 5.1% from 1986 to 1996 and 16.4% from 1996 to 2006.. Nonetheless, surface water storage in the Vea catchment has declined drastically by 52.1km^2(23.2%) from 2006 to 2020(Fig8 Y).

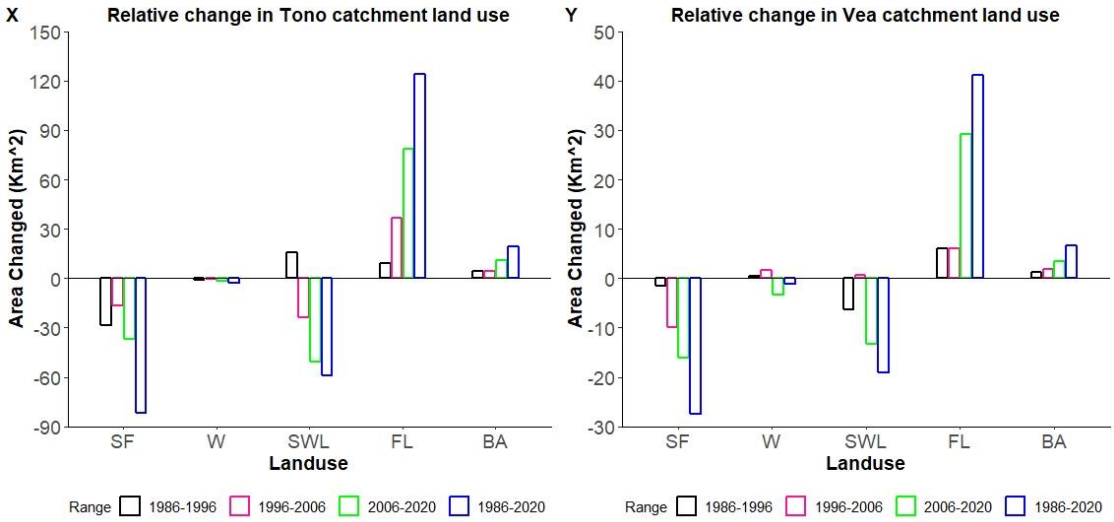

Fig 8; Relative change in land use in Tono(x) and Vea(y) catchments
Land-use change assessment based on interim year from 1986-1996(10yrs), 1996-2006(10yrs), 2006-2020(14yrs), and overall 1986 to 2020 (34yrs) respectively; negative direction denotes a decline in the magnitude of land use category in the corresponding time frame while the positive bars denote an increase in magnitude. Savannah woodland (SWL) and savannah forest (SF) generally declined consistently over subsequent decades while built areas (BA) and farmlands (FL) consistently increase in magnitude.

Table 3: Land use change assessment of Tono catchment (1986 -2020)

	1986 -1996 -2006		1996	2006-2020			1986- 2020	
Land use Category	% Δ	ARC (Km^2)	% Δ	ARC (Km^2)	% Δ	ARC (Km^2)	% Δ	ARC (Km^2)
Savannah forest	-283.9	-13.0	-164.9	-8.7	-263.3	-21.3	-240.4	-37.6
Water	-10.5	-8.5	-3.4	-3.0	-10.8	-13.7	-8.5	-23.4
Savannah wood lands	45.3	42.5	41.7	27.5	76.3	55.3	57.0	182.0

Farm land	90.9	7.5	366.7	28.2	561.2	47.2	365.7	103.0
Built area	158.2	5.9	-240.1	-8.5	-363.5	-19.7	-173.8	-22.2

Table 4; Land use change assessment of Vea catchment (1986 -2020)

	1986 -2006	-1996	1996	2006-2020		1986- 2020		
Land use Category	% Δ	ARC (Km^2)	% Δ	ARC (Km^2)	% Δ	ARC (Km^2)	% Δ	ARC (Km^2)
Savannah forest	-15.4	-3.7	-99.6	-24.9	-114.8	-53.4	-81.1	-66.2
Water	5.1	12.4	16.4	35.4	-23.2	-52.1	-3.23	-27.0
savannah woodlands	-63.2	-11.1	5.7	1.1	-95.5	-26.1	-56.2	-33.5
Farm land	60.4	22.7	59.7	18.3	208.7	75.9	121.3	155.6
Built area	13.2	10.9	17.8	13.3	24.8	22.9	19.3	54.3

Land-use Change

assessment based on the average rate of change (ARC) and percentage change(% Δ) in the magnitude of land use categories category in different time frames (1986-1996, 1996-2006, 2006-2020 and1986 to 2020) ;(-) sign denotes a decrease in the magnitude of land use category in different time frames and absolute numbers indicate an increase in the corresponding time frame

4.5 Accuracy assessment

The summary of supervised classification accuracy statistics is shown in Tables 6-9. The overall accuracy for 1986, 1996, 2006, and 2020 are 90.3%, 81.6%, 78.9%, and 94.0% respectively while respective calculated Kappa statistics results are 0.88; 0.77,0.74, and 0.92

for Tono. The calculated accuracies for Vea are 96.8%, 87.6%; 82.4%, and 98.9% for 1986, 1996, 2006, and 2020 respectively while the Kappa statistics results are 0.96, 0.84, 0.78, and 0.99 respectively. Though all image classification shows satisfactorily error margins, the 2020 images which are landsate 8 OLI/TIR images were found to have the highest classification accuracy with Kappa accuracy of 0.92 and 0.99 for Tono and Vea respectively. It's therefore clear that more advanced versions of satellite datasets improve the accuracy of classification (Poursanidis et al., 2015). Kappa coefficient is a measure of agreement between model prediction (classified image) and reality. Kappa value between 0.81 -1 denotes a near-perfect match between classified image and reference data (reality) while 0 represents complete randomness (van Vliet et al., 2011). Given the Kappa statistics of the present study ranging between 0.74 and 0.99(Table. 5-7), the scenario detection results are highly reliable to accurately inform policy and management decisions towards sustainability of the reservoirs systems from the holistic catchment perspective.

Table 6; Error matrix showing Accuracy and Kappa statistics of 1986 supervised land use classification of Tono and Vea catchments

	Tono Data								Vea Data							
Land use	Wt	CS	OS	FL	BA	TI	PA(%)	UA(%)	Wt	CS	OS	FL	BA	TI	PA(%)	UA(%)
Wt	14					14	100	100	16			1		17	100	100
CS		25		1		26	96.1	96.2		21	1	1		23	91.3	100
OS	1		2	3		26	84.6	88			19			19	100	95
FL	2	1	3	9		25	76	82.6				19		19	100	90.5
BA					22	22	100	100					16	16	94.1	100
TI	17	26	25	23	22	113			16	21	20	21	16	94		
Overall accuracy = 90.3; Kappa statistics=0.88									Overall accuracy = 96.8; Kappa statistics=0.96							

Table 7; Error matrix showing Accuracy and Kappa statistics of 1996 supervised land use classification of Tono and Vea catchment

	Tono Data								Vea Data							
Land use	Wt	CS	OS	FL	BA	TI	PA(%)	UA(%)	Wt	CS	OS	FL	BA	TI	PA(%)	UA(%)
Wt	14					14	100	93.3	13					13	100	86.7
CS	1	27	1			29	93.1	93.1		20				20	100	100

OS			2	1												
		2	5	5		42	59.5	92.6			15			15	100	78.9
FL				1												
			1	1	1	12	84.6	43.1	1		1	18	3	23	78.3	90
BA					16		100	94.1	1		3	2	12	18	66.7	80
TI		2	2	2												
	15	9	7	6	17	97			15	20	19	20	15	76		
Overall accuracy = 81.6; Kappa statistics=0.77									Overall accuracy = 87.6; Kappa statistics=0.84							

Table 8; Error matrix showing Accuracy and Kappa statistics of 2006 supervised land use classification of Tono and Vea catchments

	Tono Data								Vea Data							
Land use	Wt	CS	OS	FL	BA	TI	PA(%)	UA(%)	Wt	CS	OS	FL	BA	TI	PA(%)	UA(%)
Wt									14							
	19					19	100	100						14	93.3	100
CS		23														
			5			28	82.1	88.5		22	1	1		24	100	91.7
OS			10													
		3		6		19	52.6	41.7			17	7		24	85	70.8
FL				11												
			9			20	55	64.7			1	9	2	12	47.4	75
BA					23	23	100	100	11		1	2	13	17	86. 7	76.5
TI		2	2	1					1							
	19	6	4	7	23	109			5	22	20	19	15	91		
Overall accuracy = 78.9; Kappa statistics=0.74									Overall accuracy = 82.4; Kappa statistics=0.78							

Table 9; Error matrix showing Accuracy and Kappa statistics of 2020 supervised land use classification of Tono and Vea catchments

	Tono Data								Vea Data							
Land use	Wt	CS	OS	FL	BA	TI	PA(%)	UA(%)	Wt	CS	OS	FL	BA	TI	PA(%)	UA(%)
Wt									16							
	15					15	100	93.8						16	100	100
CS		26														
						26	100	89.7		21				21	100	100
OS			28													
	1	3				32	87.5	100			21			21	100	100
FL				26												
					2	28	92.9	96.3				19		19	95	100

BA				1	14	15	93.3	87.5				1	16	17	100	94.2
TI		2	2	2					1							
	16	9	8	7	16	116			6	21	21	20	16	94		
Overall accuracy = 94.0; Kappa statistics=0.92									Overall accuracy = 98.9; Kappa statistics=0.99							

Rows represent the categories as derived from the classified image recognized while columns represent the categories identified from the reference values in the error matrix. The diagonal of the matrices show the agreement between the classified and reference values while the off-diagonal represents the disagreement for the classified and reference values and this disagreement indicate the commission and omission error that remains between the classified and reference

5. Discussion

The present study examined sedimentation in two reservoirs in the Upper East Region of Ghana as well as the land-use change of the reservoirs watersheds. The LULCC reveals a general shift in land use towards farmlands and built areas at the disadvantage of Savanah woodlands and Savanah forest. Similar trends are reported in other studies; Gebremicael et al., (2013) in the Upper Blue Nile basin, Ethiopia, Ottinger et al., (2013) in the yellow river, China, Guan et al., (2011) in Saga, Japan, and Opoku et al.,(2019) who reported that agriculture expansion caused about 78% of tree cover removal in southern Ghana from 1986 to 2015.

The bathymetry revealed varying sedimentation rates in the two reservoir categories (small and large) which could be associated with 1) the morphologic factors of the reservoirs and 2) characteristics of the reservoir catchment that determines the sediment yield of the river flowing into it. Regarding the morphological factors, the results reveal that the Tono reservoir exhibits a lower sedimentation rate of 0.17% per annum while the Vea reservoir which is relatively smaller, fills at an annual rate of 0.304%. similar trends of sedimentation have been found in other regions of the world such as the United States where Dendy et al., (1973) found small and medium reservoirs losing storage capacity more rapidly at rates of 1.5-3.5% per annum while large reservoirs fill up with sediment at a lower rate of 0.16% per annum. Also, the largest reservoir in the United States (Lake Mead) with a storage capacity of 28,255,000acre-feet is reported to be silting at an annual rate of 0.03% (Smith et al., 1960) while Adwubi et al., (2009) also found small reservoirs in Northern Ghana silting at a high rate of 1.7%/year with some haven lost their dead storage space to sediment. The trend of larger reservoirs losing their storage space to sediment less swiftly is because more time and opportunity are available for eroded soil to deposit in the larger watershed before reaching the reservoir located downstream in a catchment. Consequently, the sediment delivery and sediment yield are likely to be lower in the larger watershed (Lane and Nichols, 1998; Birkinshaw and Bathurst, 2006). On the other hand, the sediment delivery ratio which is the percentage of eroded soil amount that reaches the watershed outlet is higher for small reservoirs since the possibility of eroded soil to get to the outlet is relatively high. Several factors impact sediment deposition in reservoirs including the drainage area and overland flow length (Hrissanthou, 2011).

Beyond the morphological factors of the reservoir, watershed characteristics reveal a more prominent decrease of forest in Vea (from 29.5% in 1986 to 9.9% 2020) while Tono watershed forest decreased from 34.7% to 21% due to the expansion of farmlands and built areas. Agriculture area expansion in reservoir watersheds has implications beyond the simple area numbers, as the removal of natural vegetation within a reservoir catchment, exposes the soil surface to rapid runoff and consequently increases the rate of particle transfer leading to higher sediments being deposited into the reservoir (Harden C.P., 1993; Liu et al., 2014). For instance, an average of 0.22% of 0.22% annual storage loss has been documented for US reservoirs with 24% of the infill sediment originating from cropland erosion (Crowder, 1987). García-Ruiz et al., (2008) also found agricultural catchments in Central Pyrenees generating twice the number of floods as that recorded in forest catchment reflected in higher sediment generation from farmlands. Though the higher sedimentation rate in Vea could be related to the size, It is also worth speculating that the sedimentation rate in Vea(small reservoir) is exacerbated by the higher change in land cover towards farmlands. Implying therefore that, though small and medium storage reservoirs lose their storage space to sediment more swiftly than larger reservoirs (Dendy et al., 1973) The severity of their vulnerability to sedimentation further depends on the watershed land cover characteristics.

5.1 Way Forward

There are several ways to deal with the sedimentation problem in reservoirs and Kondolf et al., (2014) categorized sedimentation management strategies into three; (1) reducing sediment yield from watersheds; (2) minimizing sediment deposition; and (3) recovering reservoir loss volume. Irrespective of the strategy reservoir managers seek to consider in dealing with sedimentation, examining the catchment characteristics in time and space is necessary to understand and tackle the root cause of sedimentation sustainably. the LULCC over 35 year period (1986 to 2020) suggests a fragile catchment resulting from massive removal of Savannah forest and savannah woodlands, hence implementing activities that reduce sediment production and trap sediments within the catchments of Tono and Vea is the most preferred and sustainable way to deal with reservoir sedimentation. In other related studies, Adongo et al., (2019) proposed installing a hydro-suction sediment removal system and periodic dredging of Vea and other reservoirs in Northern Ghana as a remedy to restore the fast depleting storage space. However, dredging has been proven to be expensive and in many cases environmentally damaging since it involves stirring and re-exposing buried nutrients (Kawashima, 2007). Moreover, without dealing with the high sediment yield from the watershed, de-silting may be a temporal sediment management strategy to recover volume (Kondolf et al., 2014) but not a sustainable solution.

Addressing the sediment transport problem from the upstream end could be achieved through improvement in watershed management. Strategies such as forest rehabilitation, conservation, and plantation and forest fire control should be emphasized in the management of Tono and Vea catchments. This can be achieved by advancing a holistic

catchment approach involving all relevant stakeholders including reservoir management institutions (ICOUR and IDA), MoFA, Forestry Commission, communities, and the Chiefs. The desire to expand farmlands is an attractive reason to deforest an area, hence further improving the "Taunga" system of plantation forestry introduced in the 1990's where farmers intercrop with economic trees during plantation establishment (African Development Fund, 2002) could be helpful. Thus, including fruit trees plantation in the "Taunga" system and improving the rights of farmers to better benefit sharing of economic returns when the resource is utilized, could be great incentives to improve their commitment to reforest degraded lands and afforest bare lands within the catchments. More so, this can improve the acceptability of the "Taunga" system on the part of farmers since it results in a win-win situation where farmers stand to gain financially from selling fruits while trees also reduce sedimentation. Also, developing alternatives to deforestation, adopting sustainable farming practices and new farming technologies that require less land could help in catchment restoration. Though the Forestry Commission has started community policing of forest reserves, "Fee For a Grown Tree on Bare Lands (FGTBL)" approach could be adopted since the monetary gains may motivate sustainable trees establishment in open areas and not only in designated reserves. Most importantly, dealing with the weak inter-agency coordination in planning, management, and monitoring natural resources is of critical importance to improving the resilience of the Tono catchment and restoring the fragile Vea catchment. Fortunately, the well-watered and fertile lands along the flow paths of Yarigatanga river which feeds the Vea reservoir have largely remained intact (Fig 6). Hence, there is a possibility to save the reservoir by designating those areas as forest reserves while grassing the fringes of the dam to trap sediments.

5.2 Uncertainties and limitations of the study

The uncertainties associated with the current study include; uncertainties related to bathymetry data acquisition and processing and uncertainties linked to the visual image interpretation.

1 Uncertainty linked to bathymetry data acquisition and processing; There are many sources of errors inherent in calculating changes in sediment volume from bathymetric maps collected at different times including systematic errors, blunders, and random errors (Mills 1998; HQUSACE 2002). The single-beam Ecosounder (echoMAP CHIRP 72SV) used in this study, measured depth at an accuracy of ±0.01m, which Johnston, (2002) asserts that individual points may have that precision but the overall accuracy of bathymetry analysis describing geomorphic changes may eventually be lowered due to uncertainty in the raw data. In addition, survey points were collected in a regular grid on average of 30 by 30m. Hence, random errors arising from the inability to perfectly measure the depth; natural variation in the reservoir floor at a spatial scale smaller than the sampling interval is inevitable. Another major drawback of the hydrographic survey is that, at the time of the survey, the reservoirs' water levels were not at

full supply level (FSL) and so, bathymetry data were adjusted to minimal pool level given room for possible blunders.

2 Uncertainties connected to the visual image interpretation; The unavailability of quality data for the same season for the set study years required that data be acquired from different seasons making the spatial and landscape arrangement in the satellite image a bit variant. Thus, low–laying areas (classified as farmlands in the dry season image) appear as water bodies (in the rainy season images) with water temporarily laying in such areas following rainfall incident, manifesting in the classified image as land types being allocated to the wrong class (Congalton et al., 2014). Additionally, just like other image classification studies, uncertainties related to this study from data processing and analysis include errors in ground truth data collection, geo-referencing, classification scheme, classifiers, and sampling scheme (Congalton, 1991; Hammond and Verbyla, 1996). In other to minimize the uncertainties associated with this study, enough ground truth data points were collected alongside a high sample size of the training dataset. Also, the dataset was radiometrically corrected before classification.

6. Conclusion and Recommendation

Reservoir sedimentation is variant all over the world and the extent of sedimentation depends on the physiography of the reservoir and the catchment characteristic. While there are many factors regarding the catchment characteristics, land cover change is the major controller of runoff and consequent sediment transport. The current study examined the sediment deposition rate in a large reservoir (Tono) and a small reservoir (Vea) in Ghana in relation to changes in their watersheds from 1986 to 2020 Var bathymetry and LULCC analysis. The Tono and Vea are unique in the sense that, the reservoirs are the primary source of water to the Upper East Region of Ghana and their watersheds are transboundary, shared between Ghana and Burkina Faso. The hydrographic survey in 2020 reveals an annual sedimentation rate of 0.17% and 0.304% for Tono and Vea respectively. The LULCC analysis in both catchments reveals a similar pattern of change towards agricultural expansion to the detriment of savannah forests and woodlands with a more drastic change in Vea than Tono. The relatively smaller reservoir appears to be filling up with sediment more rapidly than the larger reservoir. Since small reservoirs are known to be more vulnerable to sedimentation, the high sedimentation in the Vea reservoir could be linked to its size, exacerbated by the more rapid tree cover removal in its watershed.

According to these observations, it could be said that tree cover removal has a rippling effect on water resources. Hence greater attention needs to be given to watershed management practices through stronger collaborative efforts from the forest and water resources managers. Also, the majority of the locals interviewed confirmed the alarming tree cover removal in the catchments, especially around the Vea reservoir but are adamant about the consequences because they are only concerned about their present self-sufficiency.

Hence, an integrated forest cover-water conservation plan with the locals empowered as key stakeholders to help conserve the forest cover to extend the life of the reservoirs is necessary. This will require sensitization, capacity building by different training activities on land conservation and buffer zone issues alongside strict enforcement of buffer zone policies. Another most effective way to consider in dealing with the sedimentation challenge is the establishment of vetiver hedges to form a continuous band around the fringes of reservoirs. The extensive fibrous rooting system of the Vetiver grass (*Vetiveria zizanioides*) slows down runoff velocity, filters, and hold back sediments carried in overland flow, hence minimizing the quantity of sediment deposited in reservoirs while enhancing the groundwater table due to improved percolation.

Though the results provide a basis for understanding sedimentation dynamics in Tono and Vea to inform policy and practice towards sustainable reservoir sediment management, there are uncertainties associated with the bathymetry data acquisition and processing as well as limitations linked to the visual image interpretation. Furthermore, there are watershed characteristics that influence sedimentation apart from the reservoir physiography and watershed land cover characteristics such as geology, topographic character, climate, geomorphology, soil, and hydrology. Hence, future studies should focus on untangling the relationship between reservoir sedimentation and all catchment characteristics. This could be crucial to have a holistic understanding of the sedimentation process in these reservoirs from their catchment viewpoint. It also provides a basis for further studies on community participation in watershed management.

Acknowledgment

This study was funded by the Regional Water and Environmental Sanitation Center Kumasi (RWESCK). At the Kwame Nkrumah University of Science and Technology, Kumasi with funding from Ghana government through the World Bank under the Africa Center's of Excellence project.

Compliance with Ethical standards

Conflict of interest; The authors declare that they have no known competing financial interests or personal relationships that could have appeared to influence the work reported in this paper.

Reference

Adongo, T.A., Kyei-Baffour, N., Abagale, F.K., Agyare, W.A., 2019. Assessment of reservoir sedimentation of irrigation dams in northern Ghana. Lake Reserv. Manag. 36, 87–105. https://doi.org/10.1080/10402381.2019.1659461

Adwubi, A., Amegashie, B.K., Agyare, W.A., Tamene, L., Odai, S.N., Quansah, C., Vlek, P., 2009. Assessing sediment inputs to small reservoirs in Upper. Lakes Reserv. Res. Manag. 2009 14 279–287 279–287. https://doi.org/10.1111/j.1440-1770.2009.00410.x

African Development Fund (ADF), 2002. Appraisal Report Community Forestry Management Project Republic of Ghana.

AKE SUNDBORG, 1992. Lakes and Reservoir Sedimentation Prediction and Interpretation. Lake Reserv. Manag.

Akubia, J.E.K., Ahmed, A., Antje Bruns, 2020. Assessing How Land-Cover Change Associated with Urbanisation A ff ects Ecological Sustainability in the Greater Accra Metropolitan Area , Ghana.

Awotwi, A., Yeboah, F., Kumi, M., 2014. Assessing the impact of land cover changes on water balance components of White Volta Basin in West Africa Assessing the impact of land cover changes on water balance components of White Volta Basin in West Africa. https://doi.org/10.1111/wej.12100

Barry, B., Obuobie, E., Andreini, M., Andah, W., Pluquet, M., 2005. The Volta River basin, Assessment, Comprehensive Management, Water. Water 1–187.

Berhane, G., Gebreyohannes, T., Martens, K., Walraevens, K., 2016. Overview of micro-dam reservoirs (MDR) in Tigray (northern Ethiopia): Challenges and benefits. J. African Earth Sci. 123, 210–222. https://doi.org/10.1016/j.jafrearsci.2016.07.022

Birkinshaw, S.J., Bathurst, J.C., 2006. Model study of the relationship between sediment yield and river basin area 761, 750–761. https://doi.org/10.1002/esp.1291

Boakye, E., Anornu, G.K., Quaye-ballard, J.A., Donkor, E.A., 2018. Land use change and sediment yield studies in Ghana : Review 11, 122–133. https://doi.org/10.5897/JGRP2018.0707

Chander, G., Markham, B.L., Helder, D.L., Ali, E.-, 2009. Remote Sensing of Environment Summary of current radiometric calibration coef fi cients for Landsat MSS , TM , ETM + , and EO-1 ALI sensors. Remote Sens. Environ. 113, 893–903. https://doi.org/10.1016/j.rse.2009.01.007

Chanson, H., 1998. Extreme Reservoir Sedimentation in Australia: a Review. Int. J. Sediment Res. 13, 55–63.

Chanson, H., & James, D. P. (2005). Siltation of Australian Reservoirs: Some Observations and Dam Safety Implications. Department of Civil Engineering, The University of Queensland, Brisbane QLD 4072, Australia.

Congalton, R.G., 1991. A review of assessing the accuracy of classifications of remotely sensed data. Remote Sens. Environ. 37, 35–46. https://doi.org/10.1016/0034-4257(91)90048-B

Congalton, R.G., Gu, J., Yadav, K., Thenkabail, P., Ozdogan, M., 2014. Global land cover mapping: A review and uncertainty analysis. Remote Sens. 6, 12070–12093. https://doi.org/10.3390/rs61212070

Dendy, F.M., Champion, W.A., Wilson, R.B., 1973. Reservoir Sedimentation Surveys in the United States 17.

Dutta, S., 2016. Soil erosion , sediment yield and sedimentation of reservoir : a review. Model. Earth Syst. Environ. 2, 1–18. https://doi.org/10.1007/s40808-016-0182-y

Forest Services Division (FSD), 2015. Annual Report of the Forestry Services Department; Upper East Region; Ghana.

Fries, J., 1991. Management of Natural Forests Semiarid Areas of Africa 20, 395–400.

Fu, K.D., He, D.M., Lu, X.X., 2008. Sedimentation in the Manwan reservoir in the Upper Mekong and its downstream impacts. Quat. Int. 186, 91–99. https://doi.org/10.1016/j.quaint.2007.09.041

García-Ruiz, J.M., Regüés, D., Alvera, B., Lana-Renault, N., Serrano-Muela, P., Nadal-Romero, E., Navas, A., Latron, J., Martí-Bono, C., Arnáez, J., 2008. Flood generation

and sediment transport in experimental catchments affected by land use changes in the central Pyrenees. J. Hydrol. 356, 245–260. https://doi.org/10.1016/j.jhydrol.2008.04.013
Gebremicael, T.G., Mohamed, Y.A., Betrie, G.D., van der Zaag, P., Teferi, E., 2013. Trend analysis of runoff and sediment fluxes in the Upper Blue Nile basin: A combined analysis of statistical tests, physically-based models and landuse maps. J. Hydrol. 482, 57–68. https://doi.org/10.1016/j.jhydrol.2012.12.023
Ghana Irrigation Development, (GIDA), 2010. Final Report of the Ghana Social Opportunity Project (GSOP).
Guan, D., Li, H., Inohae, T., Su, W., Nagaie, T., Hokao, K., 2011. Modeling urban land use change by the integration of cellular automaton and Markov model. Ecol. Modell. 222, 3761–3772. https://doi.org/10.1016/j.ecolmodel.2011.09.009
Hammond, T.O., Verbyla, D.L., 1996. Optimistic bias in classification accuracy assessment. Int. J. Remote Sens. 17, 1261–1266. https://doi.org/10.1080/01431169608949085
Imagen Consult, 2013. Tono Project Water Availability Assessment, Tono Project-Ghana.
Irrigation Development Authority (IDA), 1978. Tono Irrigation project; Abrief description.
J. Fries and J.Heermans, 2014. Natural forest management in semi-arid Africa: status and research needs 1–10.
Jacobsen, T., 1997. Sediment Problems in Reservoirs; Control of sediment deposits. Norwegian University of Science and Technology (NTNU).
Johnston, B.S., 2002. Uncertainty in Bathymetric Surveys. Advances 1–25.
Kawashima, S., 2007. Conserving reservoir water storage: An economic appraisal. Water Resour. Res. 43, 1–9. https://doi.org/10.1029/2006WR005090
Kondolf, G.M., Gao, Y., Annandale, G.W., Morris, G.L., Jiang, E., Zhang, J., Cao, Y., Carling, P., Fu, K., Guo, Q., Hotchkiss, R., Peteuil, C., Sumi, T., Wang, H., Wang, Z., Wei, Z., Wu, B., Wu, C., Yang, C.T., 2014. Sustainable sediment management in reservoirs and regulated rivers: Experiences from five continents. Earth's Futur. 2, 256–280. https://doi.org/10.1002/2013ef000184
Kundu, S., Khare, D., Mondal, A., 2017. Past, present and future land use changes and their impact on water balance. J. Environ. Manage. 197, 582–596. https://doi.org/10.1016/j.jenvman.2017.04.018
Lane, J., Nichols, M., 1998. Processes controlling sediment yield from watersheds as functions of spatial scale 9838.
Liu, Y.J., Wang, T.W., Cai, C.F., Li, Z.X., Cheng, D.B., 2014. Effects of vegetation on runoff generation, sediment yield and soil shear strength on road-side slopes under a simulation rainfall test in the three gorges reservoir area, China. Sci. Total Environ. 485–486, 93–102. https://doi.org/10.1016/j.scitotenv.2014.03.053
López-serrano, P.M., Corral-rivas, J.J., Díaz-varela, R.A., 1908. Evaluation of Radiometric and Atmospheric Correction Algorithms for Aboveground Forest Biomass Estimation Using Landsat 5 TM Data 1–19. https://doi.org/10.3390/rs8050369
Lunetta, R.S., Johnson, D.M., Lyon, J.G., Crotwell, J., 2004. Impacts of imagery temporal frequency on land-cover change detection monitoring. Remote Sens. Environ. 89, 444–454. https://doi.org/10.1016/j.rse.2003.10.022
Mallick, J., Kant, Y., Bharath, B.D., 2008. Estimation of land surface temperature over Delhi using Landsat-7 ETM + 12, 131–140.
Mul, M., Obuobie, E., Appoh, R., Kankam-, K., Bekoe-obeng, E., Amisigo, B., Yaw, F.,

Ghansah, B., Mccartney, M., 2015. of the Volta River Basin.
Namara, R.E., Horowitz, L., Nyamadi, B., Barry, B., 2011. Irrigation Development in Ghana: Past experiences, emerging opportunities, and future directions. Ghana Strateg. Support Progr. GSSP Work. Pap. No. 0027 41.
Opoku, E., Macgregor, C.J., Sloan, S., Sayer, J., 2019. Deforestation is driven by agricultural expansion in Ghana ' s forest reserves 5. https://doi.org/10.1016/j.sciaf.2019.e00146
Ottinger, M., Kuenzer, C., Liu, G., Wang, S., Dech, S., 2013. Monitoring land cover dynamics in the Yellow River Delta from 1995 to 2010 based on Landsat 5 TM. Appl. Geogr. 44, 53–68. https://doi.org/10.1016/j.apgeog.2013.07.003
Ozesmi, S.L., Bauer, M.E., 2002. Satellite remote sensing of wetlands. Wetl. Ecol. Manag. 10 381–402, 2002. 381–402.
Poursanidis, D., Chrysoulakis, N., Mitraka, Z., 2015. Landsat 8 vs . Landsat 5 : A comparison based on urban and peri-urban land cover mapping. Int. J. Appl. Earth Obs. Geoinf. 35, 259–269. https://doi.org/10.1016/j.jag.2014.09.010
Qasim, M., Porembski, S., Sattler, D., Stein, K., Thiombiano, A., Lindner, A., 2016. Vegetation Structure and Carbon Stocks of Two Protected Areas within the South-Sudanian Savannas of Burkina Faso. Environments 1–16. https://doi.org/10.3390/environments3040025
Rahmani, V., Kastens, J.H., de Noyelles, F., Jakubauskas, M.E., Martinko, E.A., Huggins, D.H., Gnau, C., Liechti, P.M., Campbell, S.W., Callihan, R.A., Blackwood, A.J., 2018. Examining storage capacity loss and sedimentation rate of large reservoirs in the Central U.S. great plains. Water (Switzerland) 10, 1–17. https://doi.org/10.3390/w10020190
Richards, G.L.W. and J.M., 2006. Procedural Documentation and Accuracy Assessment of Bathymetric Maps and Area / Capacity Tables for Small Reservoirs.
Sawaya, K.E., Olmanson, L.G., Heinert, N.J., Brezonik, P.L., Bauer, M.E., 2003. Extending satellite remote sensing to local scales : land and water resource monitoring using high-resolution imagery 88, 144–156. https://doi.org/10.1016/j.rse.2003.04.0006
Schleiss, A.J., Franca, M.J., Juez, C., De Cesare, G., 2016. Reservoir sedimentation. J. Hydraul. Res. 54, 595–614. https://doi.org/10.1080/00221686.2016.1225320
Society, I.M., 1993. Land Use , Soil Erosion , and Reservoir Sedimentation in an Andean Drainage Basin in Ecuador Author (s): Carol P . Harden Geoecology of the Andes : Resource Management and Sustainable Development (May , Published by : International Mountain Society Sta 13, 176–184.
Tarela, P.A., Menéndez, A.N., 1999. A model to predict reservoir sedimentation 21, 121–133.
Tate, E.L., Farquharson, F.A.K., 2000. Simulating reservoir management under the threat of sedimentation: The case of Tarbela dam on the River Indus. Water Resour. Manag. 14, 191–208. https://doi.org/10.1023/A:1026579230560
USGS. (2020). Frequently asked questions, from USGS Water-Science School. 27 June 2021, https://www.usgs.gov/faqs/what-are-band-designations-landsat-satellites.
van Vliet, J., Bregt, A.K., Hagen-Zanker, A., 2011. Revisiting Kappa to account for change in the accuracy assessment of land-use change models. Ecol. Modell. 222, 1367–1375. https://doi.org/10.1016/j.ecolmodel.2011.01.017
Venot, J.P., de Fraiture, C., Acheampong, E.N., 2012. Revisiting dominant notions: A

review of costs, performance and institutions of small reservoirs in sub-Saharan Africa, IWMI Research Report. https://doi.org/10.5337/2012.202
Walling, D.E., 1999. Linking land use , erosion and sediment yields in river basins. Hydrobiol. 410 223–240,1999 223–240.
Wang, G., Wu, B., Wang, Z.Y., 2005. Sedimentation problems and management strategies of Sanmenxia Reservoir, Yellow River, China. Water Resour. Res. 41, 1–17. https://doi.org/10.1029/2004WR003919
Wardell, D.A., Reenberg, A., Christian, T., 2003. Historical footprints in contemporary land use systems : forest cover changes in savannah woodlands in the Sudano-Sahelian zone 13, 235–254. https://doi.org/10.1016/S0959-3780(03)00056-6
Yuan, H., Shi, Q., Xiaoying, L., Jinming, X., Dan, L., Hui, Z., 2015. Sediment management decision making of the Sanmenxia reservoir based on RESCON model 10. https://doi.org/10.5897/AJAR2015.9722